

**NATIONAL ADVISORY COMMITTEE  
FOR AERONAUTICS**

**TECHNICAL NOTE**

No. 1433

**INSTABILITY OF OUTSTANDING FLANGES SIMPLY SUPPORTED AT  
ONE EDGE AND REINFORCED BY BULBS AT OTHER EDGE**

By Stanley Goodman and Evelyn Boyd

National Bureau of Standards

**FOR REFERENCE**

**NOT TO BE TAKEN FROM THIS ROOM**



Washington

December 1947

**LIBRARY COPY**

APR 30 1993

**LANGLEY RESEARCH CENTER  
LIBRARY NASA  
HAMPTON, VIRGINIA**



3 1176 01425 8876

## NATIONAL ADVISORY COMMITTEE FOR AERONAUTICS

## TECHNICAL NOTE NO. 1433

INSTABILITY OF OUTSTANDING FLANGES SIMPLY SUPPORTED AT  
ONE EDGE AND REINFORCED BY BULBS AT OTHER EDGE

By Stanley Goodman and Evelyn Boyd

## SUMMARY

The compressive buckling stress of outstanding flanges reinforced by bulbs was determined by the torsion-bending theory for flanges having 54 shapes and a range of lengths. The edge of the flange opposite the bulb and the loaded ends were considered simply supported. The results were analyzed to determine the shape of flange that gave the greatest support to the structure to which it was attached. It was found that the flanges capable of giving the most support without torsional buckling had over-all flange widths from  $1.9\sqrt{A_F}$  to  $2.6\sqrt{A_F}$ , where  $A_F$  is the cross-sectional area of the flange.

## INTRODUCTION

Flanges reinforced with bulbs are widely used in aircraft structures to stiffen the stressed-skin cover. They are also generally used as the stiffening element of wing beams with an I-section (reference 1).

The outstanding flanges in such structures have a tendency to fail under compressive load by twisting of the flange with respect to the rest of the structure. This twisting is accompanied by a translation and rotation of the reinforcing bulb. Such a failure is intermediate between torsional instability in which no cross-sectional distortion of the structure occurs (considered by Lundquist and Fligg in reference 2) and local instability in which the lines joining component plates in the structure remain straight (considered by Lundquist, Stowell, and Schuette in reference 3).

A survey of standard aluminum-alloy extrusion shows that the shape of most reinforcing bulbs is either rectangular with a rounded end and a fillet at the junction of the bulb and the flange or circular with a fillet at the junction of the bulb and the flange. In nearly all cases the bulb is found to be fastened to one side of the flange to leave the other side flat.

In the present paper solutions are given for 54 flange sections reinforced by rectangular and circular bulbs. The buckling stress is given in each case as a function of the flange length. The various flanges are compared with respect to their effectiveness in stabilizing the structure to which they are attached.

This work was conducted at the National Bureau of Standards under the sponsorship and with the financial assistance of the National Advisory Committee for Aeronautics.

#### SYMBOLS

$A_F$	cross-sectional area of flange
$A_S$	cross-sectional area of sheet in sheet-stringer structure
$b$	flange width from base to bulb center
$b_1$	width of rectangular-type bulb from free end to center line of web
$C$	torsion-bending constant for twisting of flange about simply supported edge, with warping displacement taken as zero at simply supported edge
$E$	Young's modulus
$E'$	tangent modulus
$E_r$	reduced Young's modulus $\left( \frac{4EE'}{(\sqrt{E} + \sqrt{E'})^2} \right)$
$G$	shear modulus $\left( \frac{E}{2(1 + \nu)} \right)$
$\nu$	Poisson's ratio
$I$	moment of inertia of sheet-stringer structure for bending in plane parallel to plane of flange
$I_F$	moment of inertia of flange about its base
$I_p$	polar moment of inertia of flange cross section about simply supported edge
$I_T$	torsion constant of flange section

k	numerical factor in formula for plate-type failure
L	effective flange length
$P_{cr}$	critical Euler load of sheet-stringer structure
R	fillet radius of rectangular-type bulb, equal to $t_1$
$R_1$	fillet radius of circular-type bulb
$R_2$	bulb radius of circular-type bulb
t	flange thickness
$t_1$	thickness of rectangular-type bulb
$\sigma_{cr}$	critical stress for torsional instability

#### SHAPE OF REINFORCED FLANGES

The shapes of the reinforced flanges are shown in figure 1. They include 27 reinforcing bulbs having essentially rectangular shape and 27 having essentially circular shape.

#### ANALYSIS

The buckling load of a flange in end compression depends on the edge condition along the line of attachment to the structure and on the type of instability. The type of instability, in turn, depends on the edge conditions, dimensions, and compressive stress-strain curve of the flange.

#### Edge Conditions

The edge condition along the line of attachment to the structure was chosen as simple support. This edge condition was chosen as characteristic of a sheet-and-flange combination of optimum design, in which buckling in end compression of both sheet and flange occurs at the same load. For an explanation, reference is made to figure 2, in which A is the flange and B is the sheet.

The function of the flange in figure 2(a) is twofold. It should add enough flexural rigidity to the sheet to prevent displacement of the sheet normal to its plane along the line of attachment C and it should carry its full share of the load. Sufficient flexural rigidity can be obtained by increasing the width of the flange, but this may lead to buckling at low loads, as illustrated in figure 2(b). Collection of some of the flange material in a reinforcing bulb at the free edge of the flange will usually increase the buckling load without loss in flexural rigidity. (See fig. 2(c).)

In the optimum sheet-flange combination the sheet will buckle with a nodal line along the line of attachment C, thus offering no restraining moment to rotation of the flange about C. It follows that the flange may be regarded as simply supported at C for the buckling of such an optimum sheet-flange combination.

The edge condition along the two loaded ends was assumed as simple support also. This involves no loss in generality since it is shown in references 4 and 5 that other conditions of restraint at the loaded ends can be taken care of by using equivalent simply supported flange lengths in the same way as equivalent simply supported column lengths are used in column analysis.

#### Method of Determining Buckling Load

A convenient approximate method of determining the flange buckling load when reinforcing bulbs are present is that based on the torsion-bending theory. This theory assumes that no cross-sectional distortion takes place in the flange. In the appendix this assumption is checked for the special case of a flange of constant thickness with  $\frac{a}{b} = 2$  and  $\frac{a}{b} = 5$ , for which an exact solution is available. Figure 3 shows the transverse deflection according to the "exact" theory together with the straight line corresponding to no cross-sectional distortion. It is seen that for a flange length of five times the flange width almost no cross-sectional distortion occurs; whereas for a flange length of twice the flange width a slight amount of cross-sectional distortion occurs. The critical stresses were also computed for these flanges. The critical stress according to the torsion-bending theory differed less than 1.5 percent from that according to the exact theory. It will be assumed in the analysis that reinforced flanges buckle like flanges of constant thickness, so that the torsion-bending theory is applicable as long as the flanges are not short compared with their width.

## Torsional Instability

The critical stress for torsional instability in the elastic range is, from equation (1) of reference 2:

$$\sigma_{cr} = \frac{GI_T}{I_p} + \frac{C\pi^2 E}{I_p L^2} \quad (1)$$

It is shown in reference 5 that equation (1) gives a good approximation for the buckling stress in the plastic range if Young's modulus  $E$  is replaced by the reduced modulus

$$E_r = \frac{4EE'}{(\sqrt{E} + \sqrt{E'})^2} \quad (1a)$$

where  $E'$  is the tangent modulus for stress at which reduced modulus is desired.

If the critical stress in equation (1) is divided by the reduced modulus and Poisson's ratio is taken as  $\nu = 0.3$ , which is typical of aluminum alloy,

$$\frac{\sigma_{cr}}{E_r} = \frac{I_T}{2.6I_p} + \frac{\pi^2 C}{A_F I_p} \frac{A_F}{L^2} \quad (2)$$

The values of  $I_T$ ,  $I_p$ , and  $C$  for the flanges shown in figure 1 were computed as outlined in equations (4) to (7) of reference 5. The values of  $I_p$  and  $C$  were computed with the simply supported side of the flange as the axis of rotation. The results for an arbitrary flange thickness  $t$  are given in table 1. The constants for any other flange thickness can be computed from the conditions of geometrical similarity by noting that  $I_T$  and  $I_p$  vary with  $t^4$  and that  $C$  varies with  $t^6$ . The cross-sectional area  $A_F$  and the moment of inertia  $I_F$  of the flange about its base are also given in table 1.

Equation (2) shows that the critical stress for long flanges is controlled by the ratio  $I_T/I_p$  and that for short flanges, by the ratio  $C/A_F I_p$ . Values of these ratios are given in table 1.

The largest value of  $I_T/I_p$  was obtained for flange 46, which has a circular bulb and for which  $\frac{b}{t} = 5$ ,  $\frac{R_2}{t} = 2$ , and  $\frac{R_1}{R_2} = 0.5$ . The

largest value of  $C/A_F I_p$  was obtained for flange 9, which has a rectangular bulb and for which  $\frac{b}{t} = 15$ ,  $\frac{b_1}{t_1} = 6$ , and  $\frac{b}{b_1} = 2$ .

The flexural rigidity for bending in the plane of the flange may be measured by the ratio  $I_F/A_F^2$  given in the last column of table 1. The largest value of  $I_F/A_F^2$  was obtained for flange 39, which has a circular bulb and for which  $\frac{b}{t} = 15$ ,  $\frac{R_2}{t} = 1.5$ , and  $\frac{R_1}{R_2} = 0.5$ .

The stress ratio  $\sigma_{cr}/E_r$  for buckling by torsional instability according to equation (2) is plotted against the length ratio  $L/\sqrt{A_F}$  in figures 4 to 9. Figures 4 and 5 give stress ratios for the relatively thick flanges ( $\frac{b}{t} = 5$  and  $\frac{b}{t} = 10$ ) of type A (rectangular bulb) and figures 6 and 7 give those for the thinnest flanges ( $\frac{b}{t} = 15$ ) of type A. Figure 8 gives stress ratios for 12 of the relatively thick flanges ( $\frac{b}{t} = 5$  and  $\frac{b}{t} = 10$ ) of type B (circular bulb) and figure 9, those for the thinnest flanges ( $\frac{b}{t} = 15$ ) of type B. The results for six of the thickest flanges ( $\frac{b}{t} = 5$ ) of type B could not be plotted in figure 8, since they had values of stress ratio  $\sigma_{cr}/E_r$  greater than 0.016 for all values of  $L/\sqrt{A_F}$ . The stress ratio of these flanges decreased in the sequence 46, 49, 52, 37, 40, 43. The ratio  $L/\sqrt{A_F}$  was chosen as abscissa since it is constant for flanges of a given length and a given cross-sectional area. Comparison of ordinates for a given abscissa will, therefore, show the effect of changing the distribution of material in the flange. The buckling strengths of the flanges at first decrease rapidly with increasing flange length; they tend to approach a constant value as the flange length becomes very large.

The sequence of the flanges of type A, with the rectangular bulb, for increasing critical stress ratio  $\sigma_{cr}/E_r$  at a fixed value of  $L/\sqrt{A_F}$  changes rapidly for values of  $L/\sqrt{A_F} < 25$ . For values of  $L/\sqrt{A_F} > 25$  the critical stress ratio for the thick flanges ( $\frac{b}{t} = 5$ ) is consistently above that for flanges with  $\frac{b}{t} = 10$  and  $\frac{b}{t} = 15$ . At  $L/\sqrt{A_F} = 80$ ,  $\sigma_{cr}/E_r$  varies from 0.0014 for flange 27 to 0.0127 for flange 25.

In the case of the flanges of type B, with the circular bulb, the sequence for increasing values of  $\sigma_{cr}/E_r$  at a fixed value of  $L/\sqrt{A_F}$  remains almost unchanged for values of  $L/\sqrt{A_F} > 20$ . The critical stress

ratios for the thick flanges ( $\frac{b}{t} = 5$ ) is consistently above that for the thinner flanges ( $\frac{b}{t} = 10$  and  $\frac{b}{t} = 15$ ) for values of  $L/\sqrt{A_F} > 20$ . The critical stress ratio increases rapidly with increasing bulb radius, other conditions being equal. The effect of the fillet radius is relatively unimportant.

### Plate Instability

The critical stress ratio for flange failure due to local instability, in which the part of the flange between the base and the bulb fails as a plate, was computed from the formula

$$\frac{\sigma_{cr}}{E_r} = \frac{k\pi^2}{12(1-\nu^2)} \frac{t^2}{b^2}$$

The coefficient  $k$  was taken from table 31 on page 339 of reference 6, by assuming the flange to buckle as a plate of constant thickness, simply supported on four sides. This edge condition is approximated when a large proportion of the flange material is concentrated in the bulb or when the ratio of flange thickness to flange width is relatively small. The computed critical stresses were found to be consistently higher than those for other types of instability. It was concluded that this type of failure would not occur in the range of flange lengths considered.

### Euler Instability of Sheet-Stringer Structure

The effectiveness of the flanges in preventing instability by Euler column buckling parallel to the plane of the flange was computed as follows for a sheet-stringer structure in which the stringers consist of the flanges that are being studied. The neutral fiber of such a structure will be close to the line joining the flanges to the sheet. The buckling load of the structure is given by

$$P_{cr} = \sigma_{cr}(A_F + A_S) = \frac{\pi^2 E_r I}{L^2}$$

Rearranging terms gives

$$\frac{A_S}{A_F} = \frac{\pi^2 I}{A_F^2 \left( \frac{\sigma_{cr}}{E_r} \right) \left( \frac{L}{\sqrt{A_F}} \right)^2} - 1$$

An approximation to  $I$  is obtained in many cases by neglecting the contribution of the sheet and taking  $I$  as  $I_F$ , the moment of inertia of the flange about its base. In this case,

$$\frac{A_S}{A_F} = \frac{\pi^2 I_F}{A_F^2 \left( \frac{\sigma_{cr}}{E_r} \right) \left( \frac{L}{\sqrt{A_F}} \right)^2} - 1 \quad (3)$$

The values of  $I_F$  are given in table 1.

The most efficient flange for a given stress ratio  $\sigma_{cr}/E_r$  and length ratio  $L/\sqrt{A_F}$  will be that having the highest value of  $A_S/A_F$ . Equation (3) shows that this most efficient flange corresponds to one having the highest value of  $I_F/A_F^2$ , that is, the largest radius of gyration relative to the base of the flange for a given cross-sectional area. It must be remembered that this conclusion assumes that no other instability occurs before column failure. It rules out the flanges with large values of  $I_F/A_F^2$  which fail by torsional instability at a relatively low stress.

Approximate values of  $A_S/A_F$  for the most efficient flanges capable of resisting torsional buckling under given conditions of stress and length are given in table 2 for values of critical stress ratio  $\sigma_{cr}/E_r$  from 0.005 to 0.015 and values of length ratio  $L/\sqrt{A_F}$  from 20 to 80. The flanges are given in the table and are drawn to scale of equal area in figure 10. It was found that flanges 1 and 37 were the most efficient theoretically for high critical stress ratios and low length ratios; flange 28, for medium ratios; and flanges 3 and 47, for low stress ratios and high length ratios. The five flanges which gave the most support without torsional buckling had over-all flange widths from  $1.9\sqrt{A_F}$  to  $2.6\sqrt{A_F}$ .

#### CONCLUSIONS

The buckling strengths of the flange shapes considered were evaluated in terms of a dimensionless parameter corresponding to high torsional buckling strength for long lengths, another parameter corresponding to high torsional buckling strengths for short lengths, and a third parameter corresponding to high Euler column buckling strength of the structure to which the flange is attached. In general, flanges having high values of one of these parameters have low values of the other two.

The most stable flanges were those that combined high strength in all respects. These flanges had over-all flange widths from  $1.9\sqrt{A_F}$  to  $2.6\sqrt{A_F}$ , which correspond to a relatively compact cross section, where  $A_F$  is the cross-sectional area of the flange..

National Bureau of Standards

Washington, D. C., August 27, 1946

## APPENDIX

## BUCKLING OF A UNIFORMLY COMPRESSED RECTANGULAR PLATE

An exact solution for the buckling of a uniformly compressed rectangular plate simply supported along the loaded edges and along one edge parallel to the load and free along the other edge parallel to the load is given in reference 7. This solution states that the buckle deflection  $W$  is given by

$$W = A \sin \frac{Wx}{a} (\sinh \alpha y + B \sin \beta y) \quad (A1)$$

where

$A$  arbitrary constant governing buckle amplitude

$x$  coordinate, in direction of load with origin at one corner

$y$  coordinate transverse to direction of load with origin at one corner

$a$  length of plate

$b$  width of plate

$$\alpha = \sqrt{\frac{\pi^2}{a^2} + \sqrt{\frac{k}{a^2} \frac{\pi^4}{b^2}}}$$

$$\beta = \sqrt{-\frac{\pi^2}{a^2} + \sqrt{\frac{k}{a^2} \frac{\pi^4}{b^2}}}$$

$k = \frac{\sigma b^2 h}{\pi^2 D}$ ; factor proportional to buckling stress  $\sigma$

$$B = \frac{(a^2 \alpha^2 - \nu \pi^2) \sinh \alpha b}{(a^2 \beta^2 + \nu \pi^2) \sin \beta b}$$

$h$  thickness of plate

$D$  flexural rigidity of plate

$\nu$  Poisson's ratio (0.25)

The buckle shape was computed from equation (A1) for two plates with the following characteristics:

a/b	k	$a\alpha$	$a\beta$	$b\alpha$	$b\beta$	B
5	0.506	6.71	5.02	1.341	1.005 radians or 57.6°	3.232
2	.698	5.13	2.57	2.567	1.285 radians or 73.7°	17.74

The deflection along the transverse center line is shown in figure 3 together with a dashed straight line connecting end points for  $\frac{a}{b} = 2$ . For  $\frac{a}{b} = 5$  the transverse center line remains substantially straight under load. A plate with  $\frac{a}{b} = 5$  has, therefore, practically no cross-sectional distortion, whereas comparison with the straight line shows that a plate with  $\frac{a}{b} = 2$  has a slight amount of distortion.

## REFERENCES

1. Ramberg, Walter, McPherson, A. E., and Levy, Samuel: Strength of Wing Beams under Axial and Transverse Loads. NACA TN No. 988, 1945.
2. Lundquist, Eugene E., and Fligg, Claude M.: A Theory for Primary Failure of Straight Centrally Loaded Columns. NACA Rep. No. 582, 1937.
3. Lundquist, Eugene E., Stowell, Elbridge Z., and Schuette, Evan H.: Principles of Moment Distribution Applied to Stability of Structures Composed of Bars or Plates. NACA ARR No. 3K06, 1943.
4. Kappus, Robert: Twisting Failure of Centrally Loaded Open-Section Columns in the Elastic Range. NACA TM No. 851, 1938.
5. Ramberg, Walter, and Levy, Samuel: Instability of Extrusions under Compressive Loads. Jour. Aero. Sci., vol. 12, no. 4, Oct. 1945, pp. 485-498.
6. Timoshenko, S: Theory of Elastic Stability. McGraw-Hill Book Co., Inc. (New York), 1936.
7. Timoshenko, S: Theory of Plates and Shells. McGraw-Hill Book Co., Inc. (New York), 1940, pp. 314-317.

TABLE 1 - CONSTANTS USED IN EQUATION (2) FOR REINFORCED FLANGES SHOWN IN FIGURE 1

Reinforcing bulbs of rectangular shape												
Flange	t (in.)	b t	b <sub>1</sub> t <sub>1</sub>	b b <sub>1</sub>	I <sub>T</sub> (in. <sup>4</sup> )	I <sub>P</sub> (in. <sup>4</sup> )	C (in. <sup>6</sup> )	A <sub>F</sub> (in. <sup>2</sup> )	I <sub>F</sub> (in. <sup>4</sup> )	$\frac{I_T}{I_P}$	$\frac{C}{I_P A_F}$	$\frac{I_F}{A_F^2}$
1	0.2	5	2	2	0.006381	0.207639	0.009181	0.331706	0.197699	0.03076	0.1334	1.7968
2	.1	10	2	2	.002787	.171985	.008987	.231706	.162803	.01620	.2255	3.0324
3	.12	15	2	2	.023884	1.682248	.304966	.642728	1.586931	.01419	.2821	3.8415
4	.40	5	4	2	.050185	2.186560	.322563	1.056706	2.097994	.02295	.1396	1.8789
5	.16	10	4	2	.004733	.670553	.081296	.420292	.638325	.00706	.2883	3.6136
6	.08	15	4	2	.000904	.188719	.014411	.188414	.178660	.00479	.4052	5.0327
7	.24	5	6	2	.005734	.234849	.010501	.349073	.226593	.02441	.1282	1.8596
8	.12	10	6	2	.000947	.164131	.009921	.205073	.157113	.00577	.2948	3.7359
9	.08	15	6	2	.000433	.140842	.009862	.157073	.133952	.00308	.4458	5.4293
10	.24	5	2	3	.007495	.265232	.005935	.372292	.259951	.02826	.0601	1.8755
11	.12	10	2	3	.001913	.193323	.005354	.228292	.189391	.00989	.1214	3.6339
12	.08	15	2	3	.001209	.169649	.005296	.180292	.165871	.00713	.1732	5.1029
13	.24	5	4	3	.005667	.201175	.003504	.329073	.197776	.02817	.0529	1.8264
14	.12	10	4	3	.000880	.130457	.002923	.185073	.128296	.00674	.1210	3.7456
15	.08	15	4	3	.000367	.107168	.002865	.137073	.105136	.00342	.1949	5.5956
16	.36	5	6	3	.027570	.912754	.029686	.709073	.898838	.03020	.0459	1.7877
17	.18	10	6	3	.003756	.555839	.023072	.385073	.548108	.00676	.1077	3.6964
18	.12	15	6	3	.001292	.438301	.022408	.277073	.431198	.00295	.1844	5.6168
19	.24	5	2	4	.006166	.209672	.002330	.335414	.207017	.02942	.0332	1.8401
20	.12	10	2	4	.001173	.138462	.001749	.191414	.137086	.00847	.0660	3.7415
21	.08	15	2	4	.000566	.115013	.001691	.143414	.113776	.00492	.1024	5.5318
22	.48	5	4	4	.087645	2.780794	.099960	1.244413	2.748332	.03151	.0289	1.7748
23	.24	10	4	4	.012033	1.652033	.062801	.668413	1.639172	.00728	.0569	3.6689
24	.16	15	4	4	.004233	1.280315	.059065	.476415	1.269452	.00331	.0968	5.5930
25	.24	5	6	4	.005364	.162182	.001278	.303268	.160364	.03308	.0260	1.7436
26	.12	10	6	4	.000704	.091756	.000697	.159268	.091154	.00767	.0477	3.5935
27	.08	15	6	4	.000222	.068565	.000639	.111267	.068083	.00324	.0838	5.4993



TABLE 1 - CONSTANTS USED IN EQUATION (2) FOR REINFORCED FLANGES SHOWN IN FIGURE 1 - Concluded

Reinforcing bulbs of circular shape												
Flange	t (in.)	$\frac{b}{t}$	$\frac{R_2}{t}$	$\frac{R_1}{R_2}$	$I_T$ (in. <sup>4</sup> )	$I_P$ (in. <sup>4</sup> )	C (in. <sup>6</sup> )	$A_F$ (in. <sup>2</sup> )	$I_F$ (in. <sup>4</sup> )	$\frac{I_T}{I_P}$	$\frac{C}{I_P A_F}$	$\frac{I_F}{A_F^2}$
28	0.10	5	1.0	0.5	0.0003004	0.010690	0.00003557	0.073860	0.010495	0.02810	0.04505	1.9238
29	.10	10	1.0	.5	.0004671	.058090	.0001673	.123860	.057858	.00804	.02326	3.7714
30	.10	15	1.0	.5	.0006337	.167430	.0004170	.173860	.167150	.00379	.01433	5.5298
31	.20	5	1.0	1.0	.004807	.172235	.001427	.297473	.169101	.02791	.02785	1.9110
32	.20	10	1.0	1.0	.007473	.935830	.006496	.497473	.932030	.00799	.01395	3.7661
33	.20	15	1.0	1.0	.010140	2.694380	.016556	.697473	2.689905	.00376	.00881	5.5294
34	.20	5	1.0	1.5	.004807	.173475	.002180	.299649	.170301	.02771	.04194	1.8967
35	.20	10	1.0	1.5	.007473	.942460	.010652	.499649	.938630	.00793	.02262	3.7598
36	.20	15	1.0	1.5	.010140	2.710770	.026860	.699649	2.706258	.00374	.01416	5.5285
37	.20	5	1.5	.5	.014796	.343687	.015668	.446530	.325387	.04305	.10209	1.6319
38	.20	10	1.5	.5	.017462	1.556624	.067334	.646530	1.537663	.01122	.06691	3.6786
39	.20	15	1.5	.5	.020129	4.062619	.157173	.846530	4.042998	.00495	.04570	5.6418
40	.20	5	1.5	1.0	.014796	.347013	.011470	.454509	.328508	.04264	.07272	1.5902
41	.20	10	1.5	1.0	.017462	1.577876	.058254	.654509	1.558705	.01107	.05641	3.6386
42	.20	15	1.5	1.0	.020129	4.117756	.143669	.854509	4.097920	.00489	.04083	5.6122
43	.20	5	1.5	1.5	.014796	.350120	.010742	.462736	.331342	.04226	.06630	1.5474
44	.20	10	1.5	1.5	.017463	1.598770	.056817	.662736	1.579334	.01096	.04831	3.5958
45	.20	15	1.5	1.5	.020129	4.172910	.142266	.862736	4.152804	.00482	.03952	5.5794
46	.20	5	2.0	.5	.042115	.622464	.039032	.665575	.556331	.06766	.09421	1.2559
47	.20	10	2.0	.5	.044782	2.489556	.201076	.865575	2.422756	.01799	.09331	3.2337
48	.20	15	2.0	.5	.047449	6.087797	.504703	1.065575	6.020331	.00779	.07780	5.3022
49	.20	5	2.0	1.0	.042115	.627658	.033592	.683707	.560860	.06710	.07828	1.1998
50	.20	10	2.0	1.0	.044782	2.530823	.187101	.883707	2.463341	.01769	.08366	3.1543
51	.20	15	2.0	1.0	.047449	6.201383	.476690	1.083707	6.133235	.00765	.07093	5.2223
52	.20	5	2.0	1.5	.042115	.632178	.034417	.702006	.564469	.06662	.07755	1.1454
53	.20	10	2.0	1.5	.044782	2.569360	.188689	.902006	2.500986	.01743	.08142	3.0739
54	.20	15	2.0	1.5	.047449	6.310553	.494622	1.102006	6.241514	.00752	.07113	5.1395

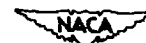


TABLE 2- DIMENSIONLESS RATIOS FOR MOST EFFICIENT FLANGES

$\frac{\sigma_{cr}}{E_r}$	0.015		0.013		0.011		0.009		0.007		0.005	
	Flange	$A_B/A_F$										
20	1	2.0	1	2.4	--	---	--	---	--	---	--	---
30	37	.2	37	.4	28	0.9	28	1.4	3	5.3	--	---
40	--	---	--	---	28	.1	28	.3	3	2.4	3	3.7
50	--	---	--	---	--	---	--	---	47	.8	3	2.0
60	--	---	--	---	--	---	--	---	47	.3	3	1.1
70	--	---	--	---	--	---	--	---	--	---	3	.6
80	--	---	--	---	--	---	--	---	--	---	3	.2



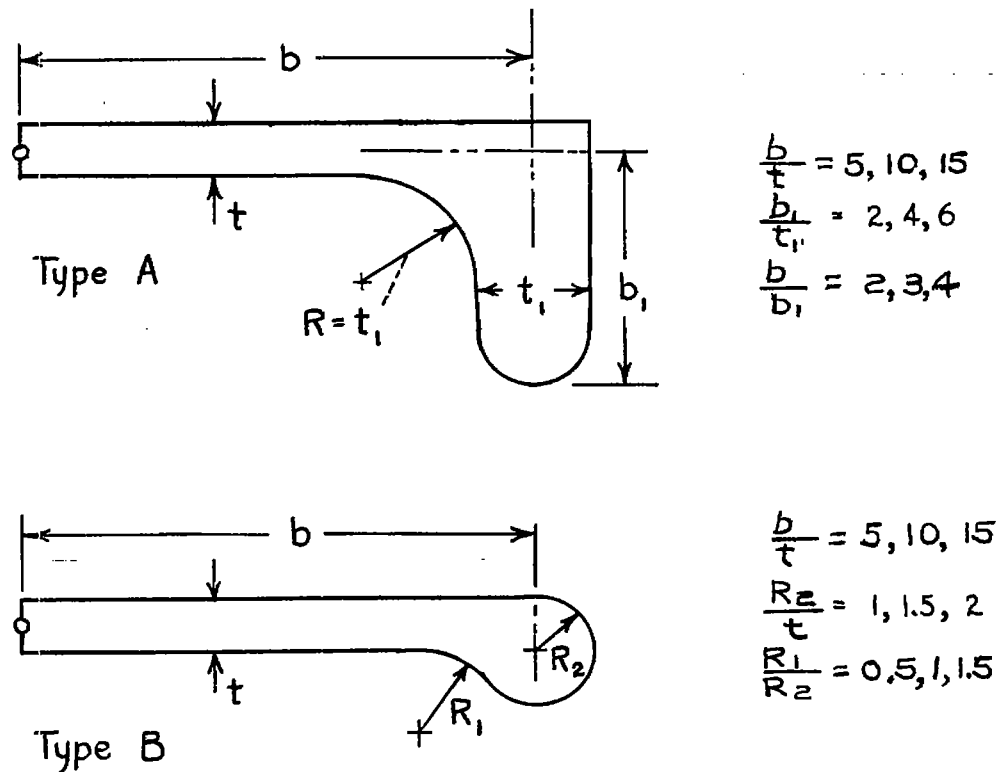


Figure 1.- Shapes of reinforced flanges.

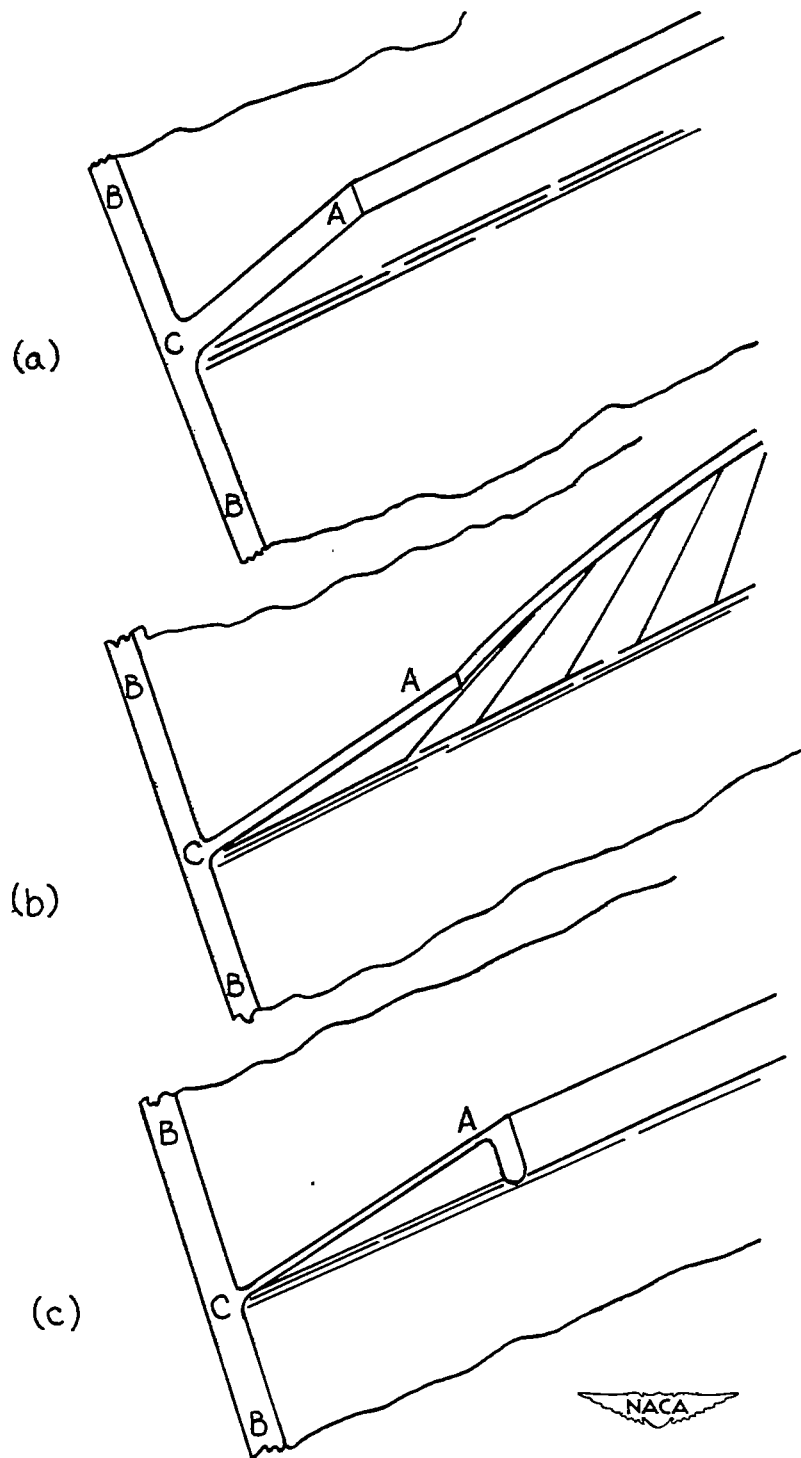


Figure 2.- Sheet-flange configurations.

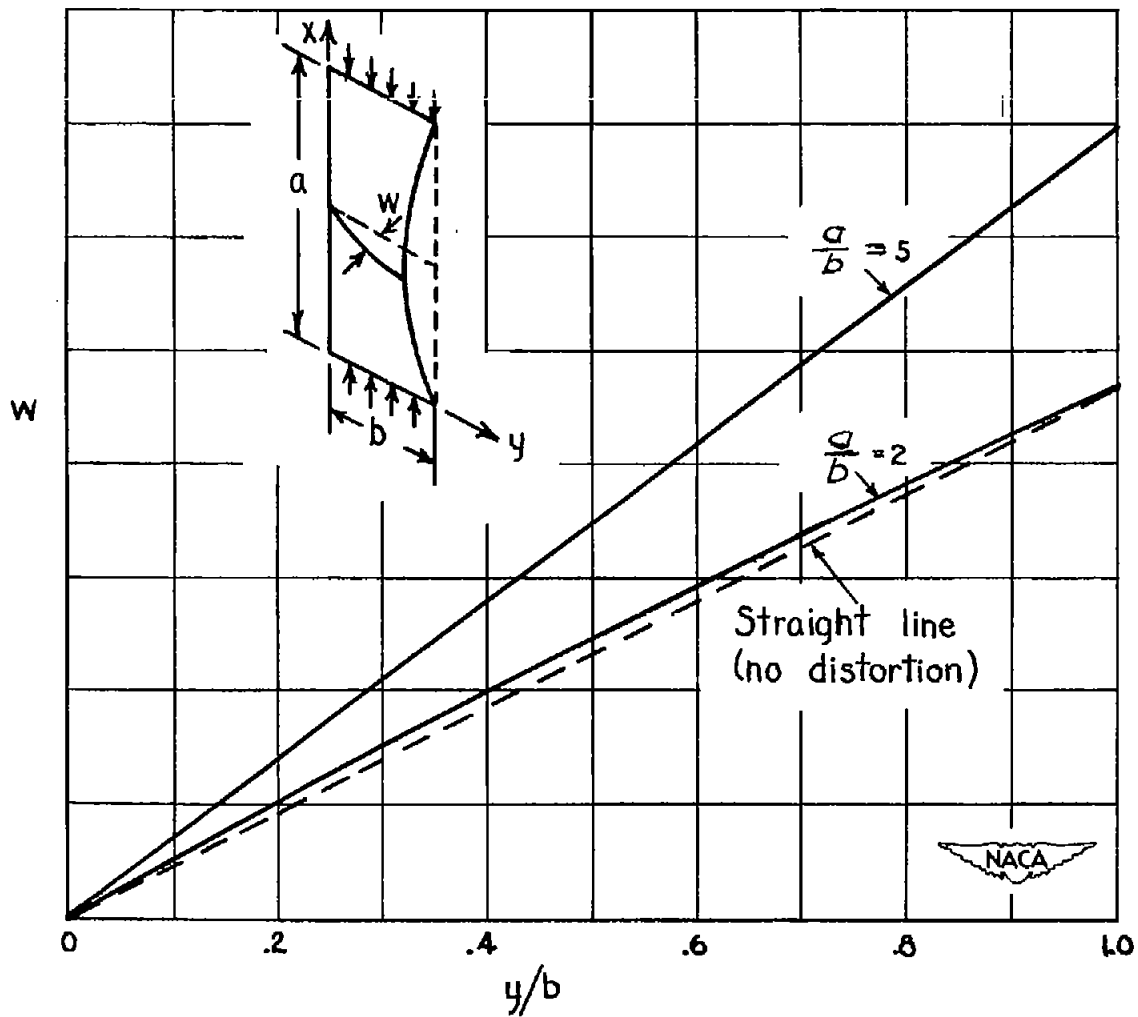


Figure 3.- Amplitude of transverse deflection for flange of constant thickness.

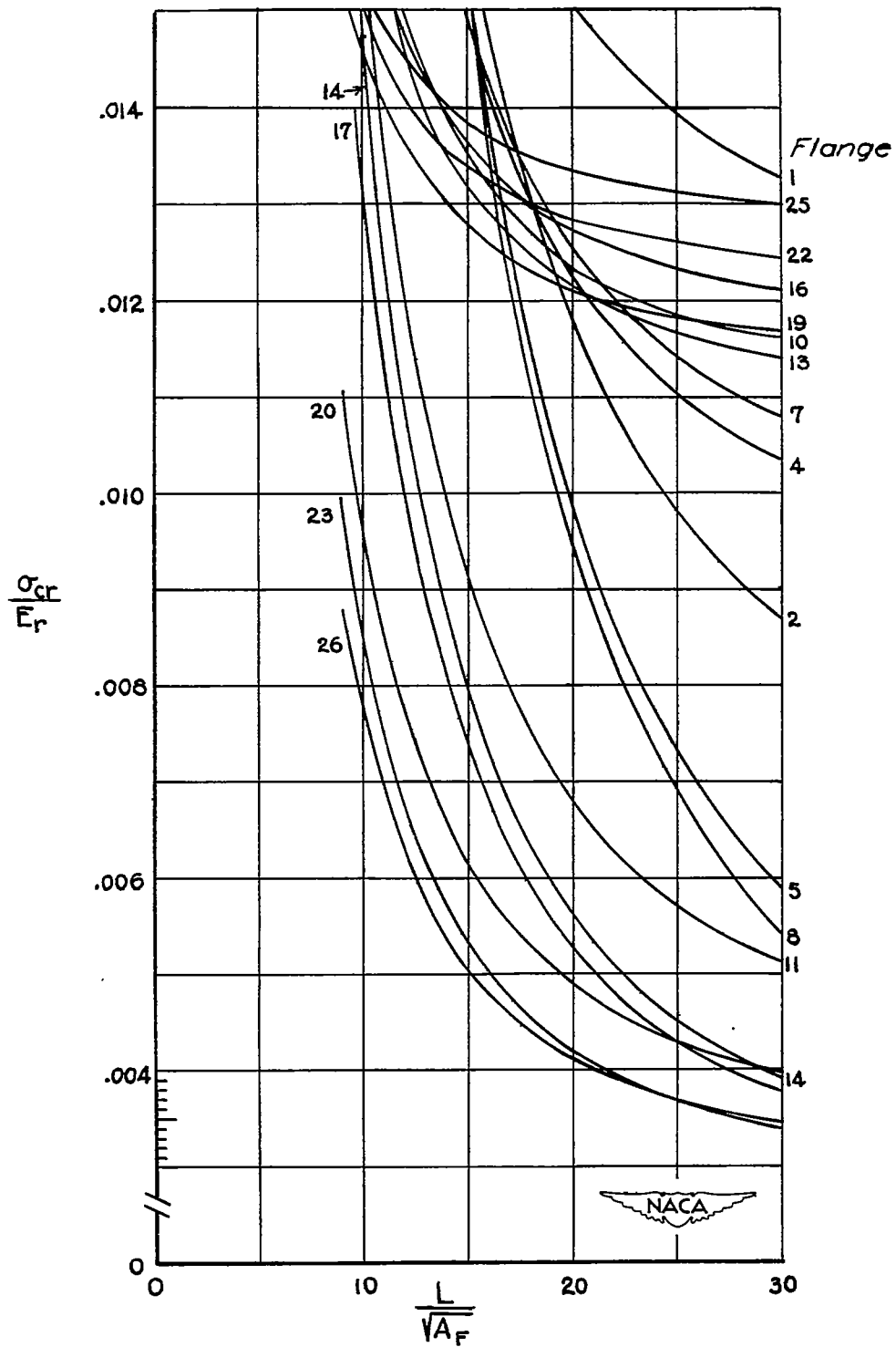


Figure 4.- Torsional buckling strength of flanges of type A.

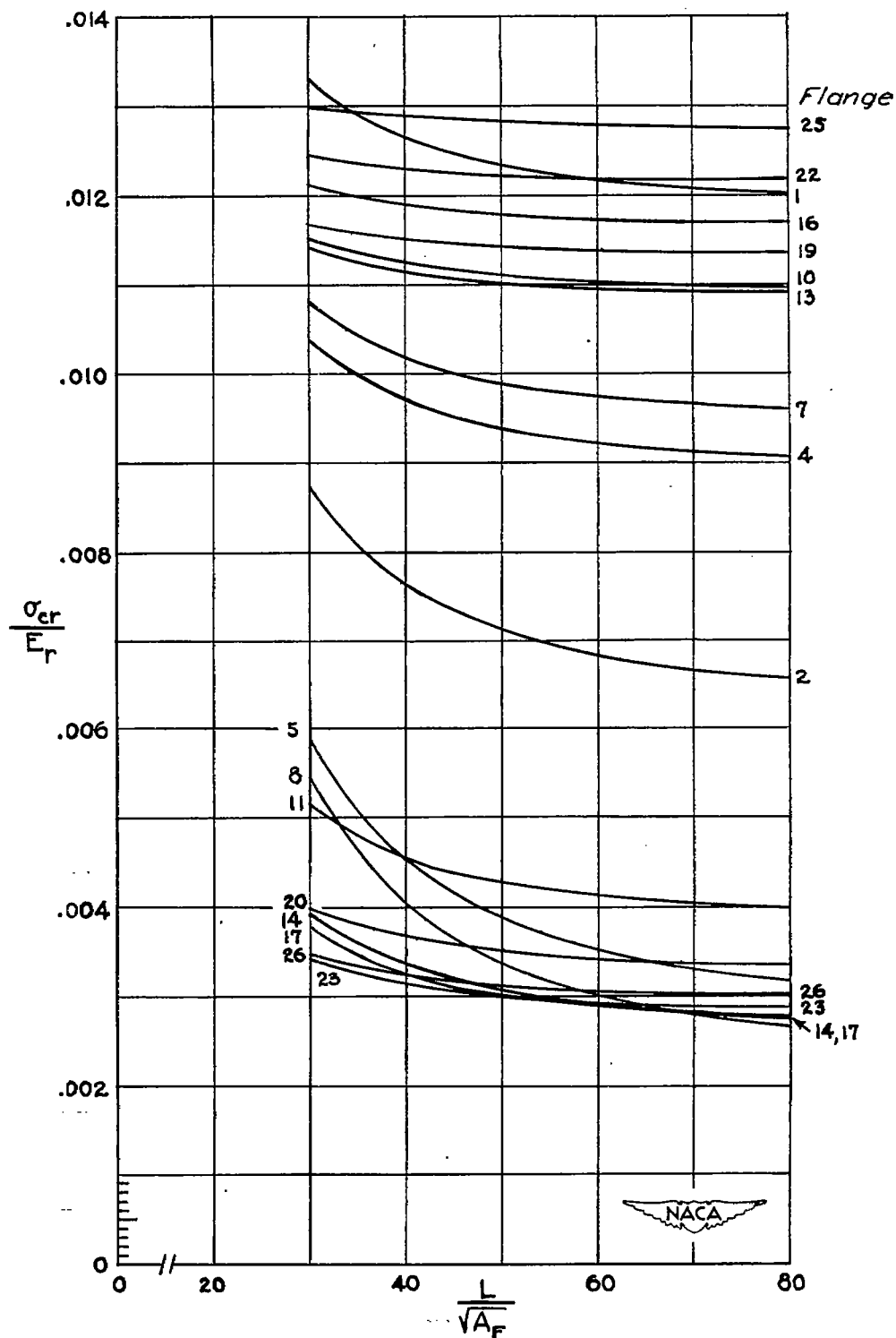


Figure 5.- Torsional buckling strength of flanges of type A.

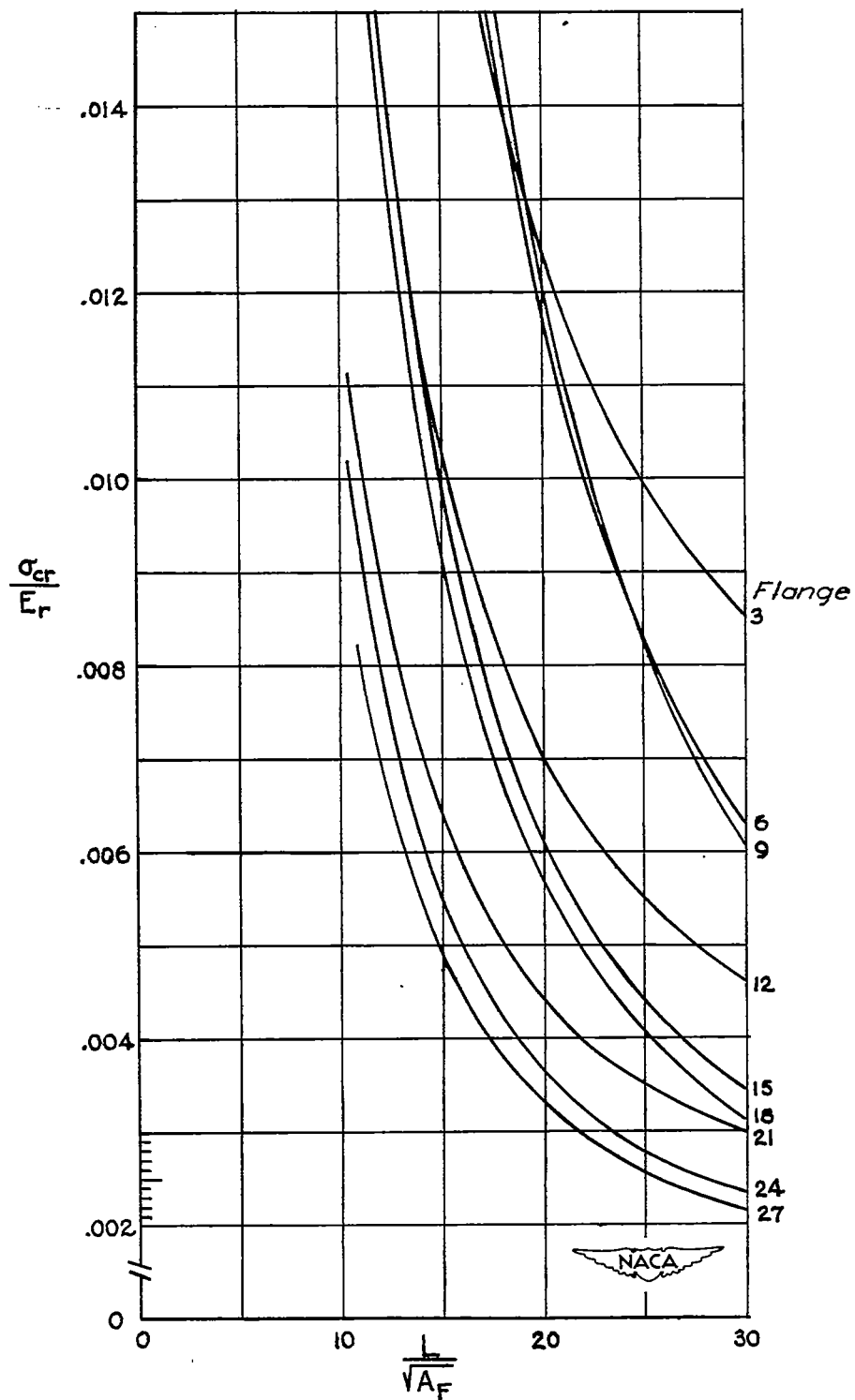


Figure 6.- Torsional buckling strength of flanges of type A.

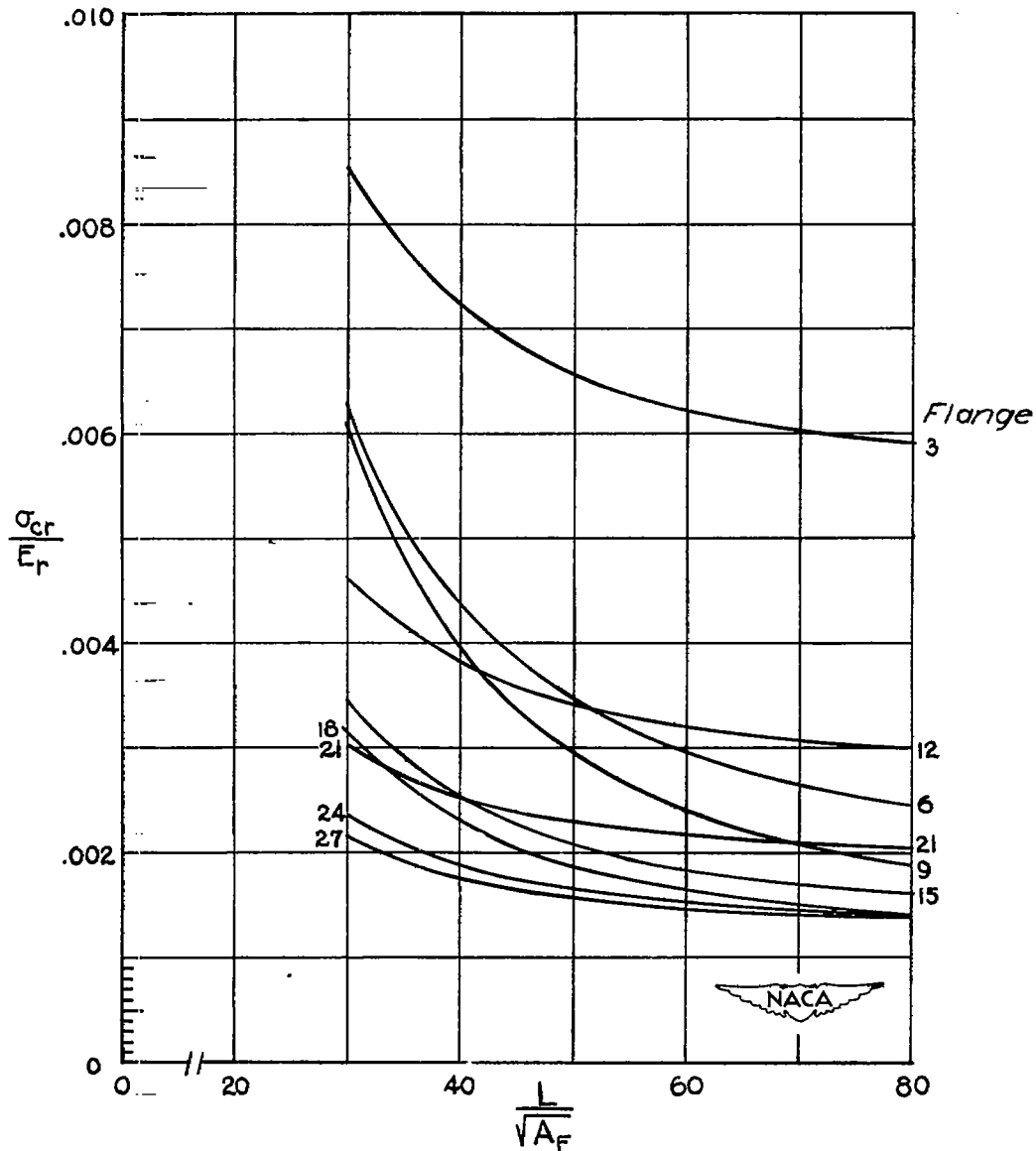


Figure 7.- Torsional buckling strength of flanges of type A.

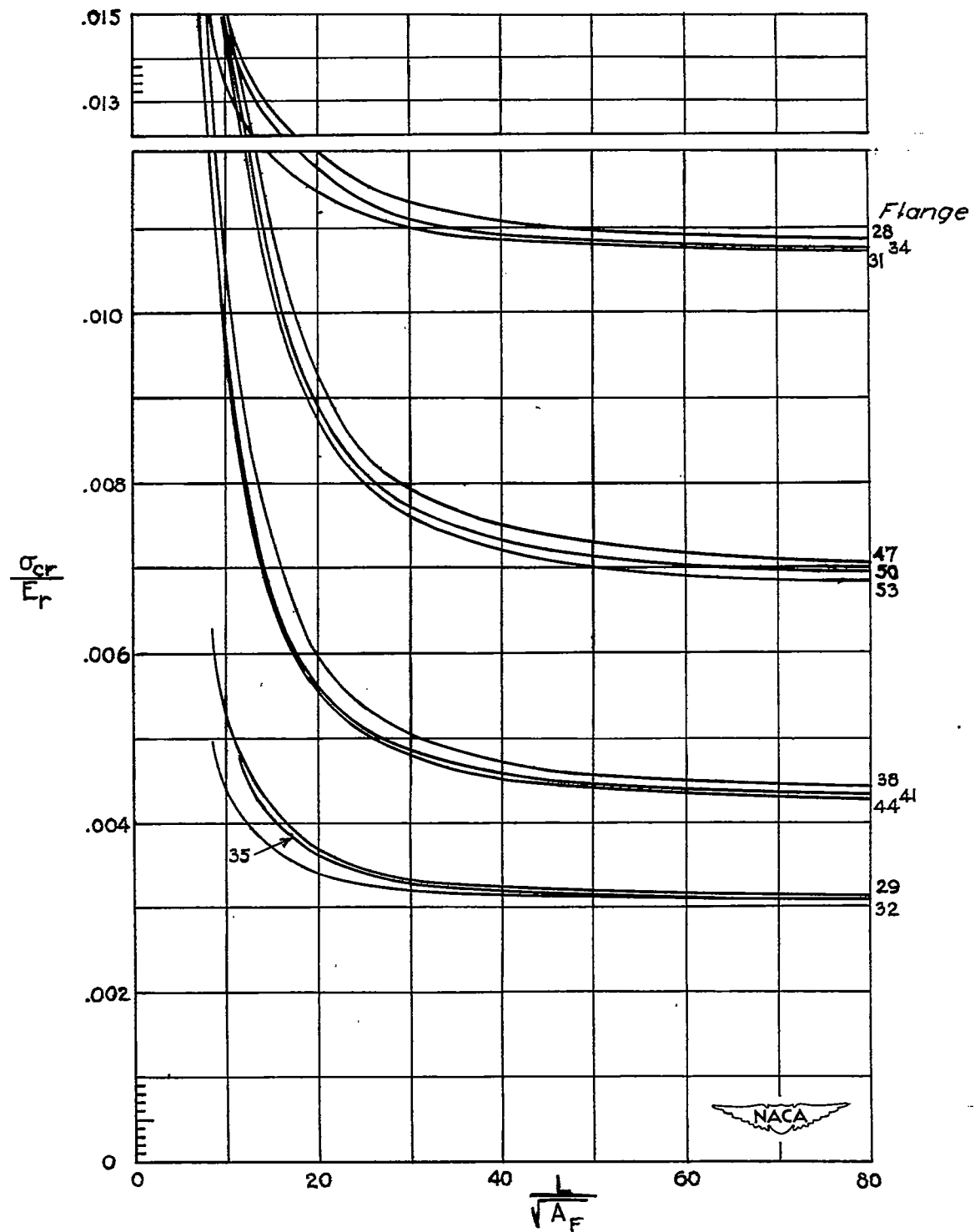


Figure 8.- Torsional buckling strength of flanges of type B.

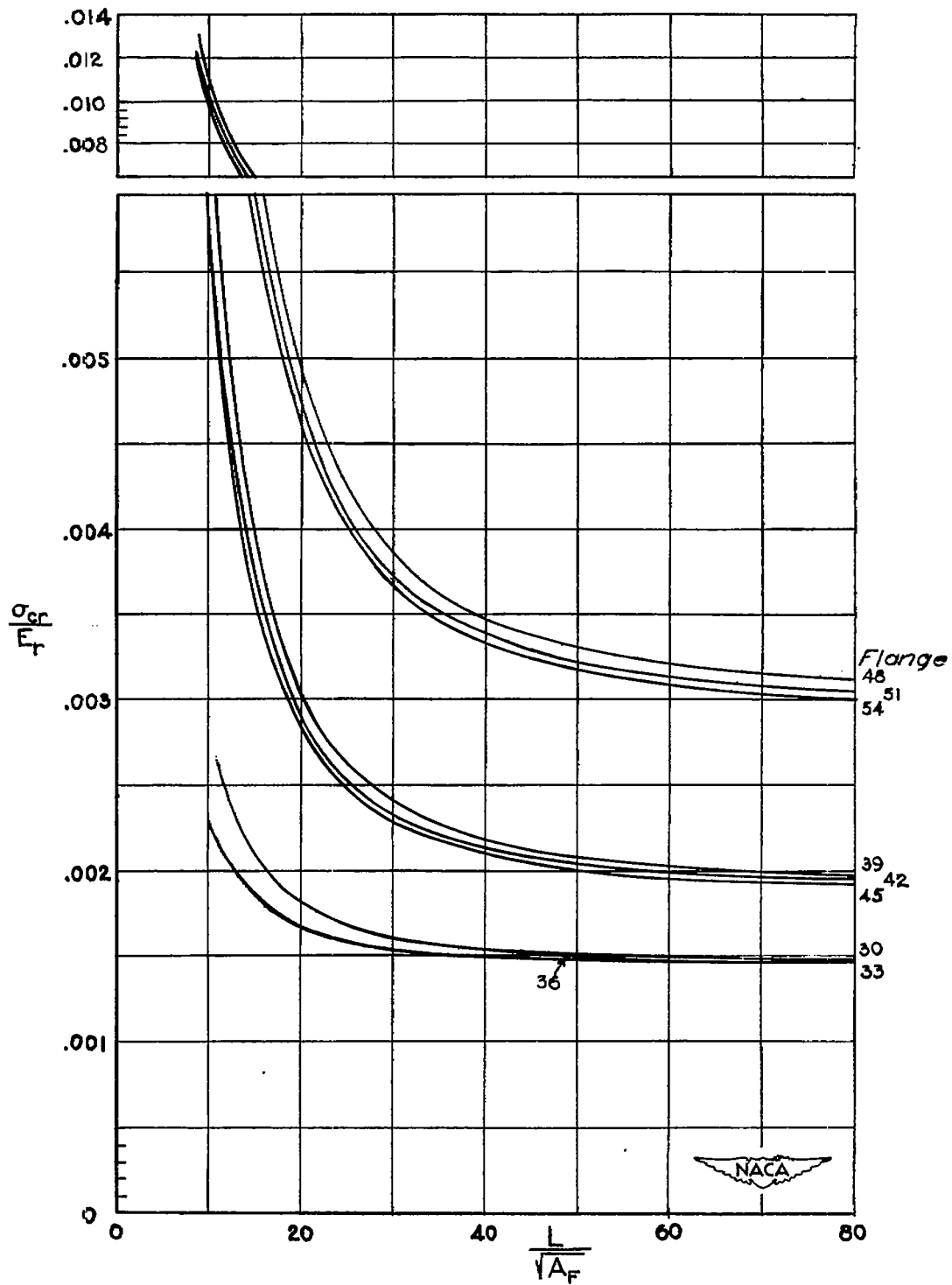


Figure 9.- Torsional buckling strength of flanges of type B.

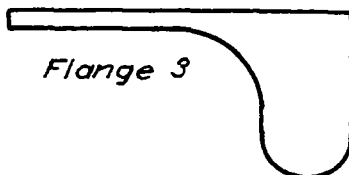
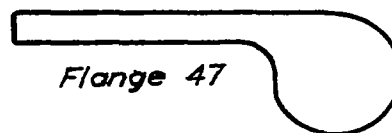
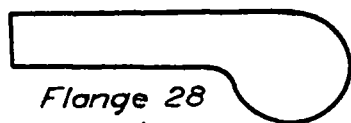
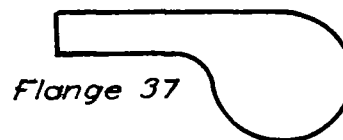


Figure 10.- Most stable flanges drawn to scale of equal area.